

Grain Profile of a Printing System

Chunghui Kuo, Yee Ng, and Di Lai; Graphic Communications Group, Eastman Kodak Company; Rochester, NY 14653, USA

Abstract

Perceived color graininess is an important image artifact affecting image quality of a digital printing system, which can be attributed to various parts of a digital printing system such as colorant physical properties, digital halftone design, etc. The conventional approach to quantifying color granularity on a printing system is to conduct measurements on individual color channels. While this is an effective way to measure each color channel's influence on color granularity, it fails to quantify the overall impact in reality where most of the image is composed of more than one colorant. Furthermore, it is possible to optimize the overall system performance in terms of color graininess if the cross interaction among different color channels is known. In this paper, we propose to create a multidimensional grain profile in the Profile Connection Space (PICS) to describe the entire system performance in perceived color graininess.

Introduction

Perceived color graininess is one of the image artifacts affecting the image quality of a digital printing system, and it can be attributed to various parts of the digital printing system, such as photoconductor, colorant physical properties, digital halftone design, etc.. The prevalent approach to quantify the quality impact of color granularity on the printing system is to measure color granularity on each individual color channel. While this is an effective way to measure each color channel's influence on color granularity, it fails to quantify the actual impact more accurately because most of the images are composed of more than one colorant. For example, adopting a less aggressive black replacement strategy will improve the image quality in terms of perceived color graininess. Simply measuring granularity on one color channel will not reveal this advantage; however, it is well known that the stability of neutral color rendition will suffer under an excessively conservative black replacement strategy. As a result, it is possible to optimize the overall system performance with respect to color rendition and color graininess simultaneously if the cross interaction among different color channels is known. Similar to the color profile characterizing the color rendition of a printing system, we propose in this paper to create a multidimensional grain profile in the Profile Connection Space (PICS) to describe the system performance in color graininess.

The process of creating the grain profile is very similar to building an ICC color profile. The first step is to define a target sampling the entire color gamut of the printing system with a lower bound on the size of the patches determined by the physical constraint to accurately quantify color granularity. The flatbed scanner is adopted as the measurement device because of its capability to capture large areas in high resolution. An automatic patch location algorithm is devised to complete the process with minimal user intervention. The automatic screen removing algorithm based on short-time Fourier transform is applied on each

segmented color patch, and we can measure the color granularity on the corresponding descreened color patch [1]. The last step is to construct a multidimensional lookup table denoted as the grain profile of the printing system mapping from either printer device grid or CIELAB color grid to the estimated color graininess based on the sampling points. If the CIELAB color grid is chosen, the derived grain profile is implicitly associated with a specific color profile and rendering intent when the target is printed because different black replacement strategy and color interpretation will impose different degrees of impact on color granularity. For instance, the gamut mapping strategies are usually different between the colorimetric intent and the perceptual intent [2]. As a result, the same color in the PCS will often be rendered differently, and this in turns results in a different amount of perceived color graininess.

In this paper, we will first propose a global grain profile model derived from the assumption of two factors contributing to the perceived color graininess on prints, i.e., colorant color contrast and the irregularity of halftone screen dot structure. We will demonstrate that combining both factors will be sufficient to explain a significant portion of the variation of the estimated color graininess within the gamut of a printing system. A supplemental generalized regression neural network is adopted to model the remaining color graininess variation. CIELAB is selected as our working color space instead of the printer's intrinsic device space such that the designed target can be applicable to any printer regardless of the number of available color channels. Our numerical experiment will verify our proposed grain profile model under various types of halftone screens and processes.

Grain Profile Model

We extend the definition of color graininess as the aperiodic chromatic/luminance noise perceived on a printed sample with spatial frequency above 0.4 cycles/mm and viewing distance being 30 cm, which is based on the definition provided by ISO/IEC 13660 [1, 3]. That is to say, the perceived color graininess can be attributed as noise with high spatial frequency content. Thus, the microscopic image structure plays a dominant role in determining the level of the noise perceivability. Consequently, analyzing the microstructure on a printed halftone image is essential to explaining the estimated color graininess of the printing system across the entire color gamut. Figure 1 shows two perfect theoretical cluster-dot halftone structures before and after the midtone density point where a dot-pattern and a hole-pattern are formed respectively. Denote the substrate area as Γ_s , the area covered by colorant as Γ_t , and its peripheries as $\partial\Gamma_t$. Assigning the location of the center of each dot/hole as (u_i, v_i) and the radius as R , $\partial\Gamma_t$ can be represented as follows:

$$\partial\Gamma_t(\theta, R) = \bigcup_i \{(u_i, v_i) + R(\cos \theta, \sin \theta)\}. \quad (1)$$

It can be easily shown that $\partial\Gamma_t$ is infinitely differentiable in $[0, 2\pi)$ and it is a linear function of R . Constrained by the limited resolution of a real printing system, $\partial\Gamma_t$ is replaced by a collection of piecewise smooth closed curves, $\partial\Gamma_d(\theta, R)$, of which infinite differentiability no longer holds [4]. Furthermore, we assume that the noise during the entire imaging process will manifest itself as an isotropic random noise term, $N_p(R)$, which is independent from θ . As a result, the peripheries of actual printed halftone patterns, $\partial\Gamma_a(\theta, R)$, can be decomposed into two terms:

$$\partial\Gamma_a(\theta, R) = \partial\Gamma_d(\theta, R) + N_p(R). \quad (2)$$

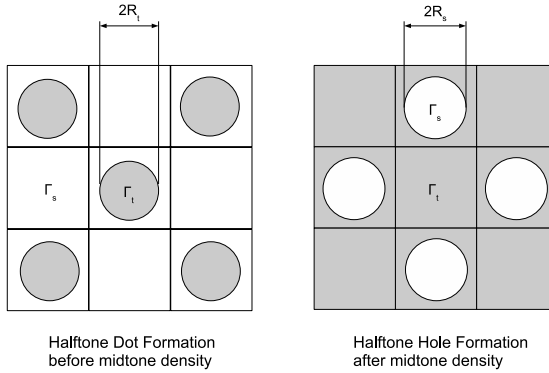


Figure 1. Perfect cluster dot structure

Γ_s , Γ_t , and $\partial\Gamma_a$ are disconnected, and $\{\Gamma_s, \Gamma_t, \partial\Gamma_a\}$ composes the entire viewing area. Thus, we can assume that the overall color graininess, VG , perceived on a printed image is the sum of contribution from each factor shown as follows:

$$VG = g(\Gamma_s) + g(\Gamma_t) + g(\partial\Gamma_a). \quad (3)$$

Let ζ_s represent the noise perceived on the adopted substrate, and ζ_t be the color graininess under complete coverage. Assuming λ as the ratio of area occupied by Γ_t , we can easily simplify Equation (3) to be the following:

$$VG = (1 - \lambda)\zeta_s + \lambda\zeta_t + g(\partial\Gamma_a) \quad (4)$$

where $(1 - \lambda)\zeta_s + \lambda\zeta_t$ is a linear function connecting ζ_s and ζ_t . Since $\partial\Gamma_d$ is a set of piecewise smooth closed curves, their contribution to color graininess is negligible. Thus, Equation (4) can be further refined to become the following:

$$VG = (1 - \lambda)\zeta_s + \lambda\zeta_t + g(N_p(R)). \quad (5)$$

Transform the closed two-dimensional curve $N_p(R)$ into a one-dimensional curve represented by signal amplitude ρ_s , frequency composition ω_s , and signal length $L_s = 2\pi R_t$, or $2\pi R_s$. After correlating with physical appearance, we propose the following three conjectures:

1. ρ_s is proportional to the color difference between Γ_s and Γ_t .
2. ω_s is determined by the chosen printing process.
3. $g(N_p)$ is a linear function of L_s .

As a result, the estimated color graininess of a primary color under a selected printing process is solely controlled by L_s . Note that the luminance component in ρ_s plays a much more significant role than the chromatic component in perceived color graininess because of the inherent human insensitivity toward high-frequency chromatic variation [5]. Based on these conjectures, we can deduce:

1. The higher the luminance contrast between Γ_s and Γ_t , the higher the perceived color graininess under the same printing process and halftone screen.
2. For a regular cluster-dot halftone screen, the color graininess should exhibit first increasing then decreasing characteristics, and reaches the highest point at the midtone density when the halftone dot formation converges with the hole formation.

The theoretical area coverage A_{th} is equal to πR_t^2 , where R_t is the radius of each dot during the halftone dot formation. However, the Yule-Nielsen model indicates that the computed area coverage, A_{comp} , as in Equation (6), is equivalent to or higher than the theoretical area coverage, A_{th} :

$$A_{comp} = \frac{1 - 10^{-D_h/n}}{1 - 10^{-D_s/n}}, \quad (6)$$

where D_h and D_s are the optical reflection density on the halftone and solid area, and n is the Yule-Nielsen value [6]. $A_{comp} \rightarrow \frac{D_h}{D_s} = A_{th}$ when $n \rightarrow \infty$, as described by Beer-Lambert-Bouguer law. As a result, after the printer density calibration process, our analysis indicates that the highest color graininess point along a primary color occurs near the 50% mark if $n \rightarrow \infty$; however, the maximal color graininess point will move to a higher percentage mark when n decreases. Lastly, the maximal color graininess point along a multi-color ramp will move forward because of the increased length of overall dot periphery.

Numerical Modeling

Analytically modeling the physical properties of a printing system relating to color graininess as explained previously is a very challenging task. Thus, we propose to describe the characteristic of color graininess of a printing system via a hybrid numerical model combining a global quadratic multidimensional polynomial and a generalized regression radial basis network [7]. We propose to adopt *CIELAB* as the working color space to be applicable to any printer. Thus, a printer output profile needs to be used to interpret these values into device colorant coverage combination, which imposes a certain complementary color replacement strategy, such as *GCR* and *UCR*, as well as the rendering intent. As a result, the estimated color grain profile for the targeted printing system is directly associated with the selected printer output profile. Along with the *CIELAB* sampling points, we also suggest to include device *CMYK*, and the two and three combinations, i.e., *Red*, *Green*, *Blue*, and *three-color Black*, for their simplicity in analysis.

The previous analysis indicates that the color graininess will reach maximum near the midtone density region depending on n , and monotonically decrease toward 0% and 100% coverage points. Thus, we found that the global behavior of color graininess within the printer color gamut can be roughly approximated

by a quadratic polynomial with all cross terms. The residual component caused by the nonlinear Yule-Nielsen effect and complicated multi-half-tone structure will be modeled by a nonparametric generalized regression radial basis network.

We adopt the same *CIELAB* space defined in *ICC* standardization with L^* , a^* , and b^* ranging from $[0,100]$, $[-128,128]$, $[-128,128]$ respectively [2]. Thus, a significant portion of the grid points are outside the actual printer gamut. To construct a color grain profile in *CIELAB*, we suggest to first apply the same printer *ICC* profile and rendering intent as the one adopted in printing the test targets from *PCS* to *device color space* then back to *PCS*. This process will guarantee that all grid points lie inside the printer gamut and a consistent complementary color replacement scheme is adopted. Finally, the resulting *CIELAB* values of the transformed sampling grid are adopted in the color graininess function derived previously to construct the three-dimensional color grain profile.

Numerical Experiment and Analysis

A five-page test target with 960 patches including *CIELAB* and *Device CMYK* color specifications is printed on a four-color

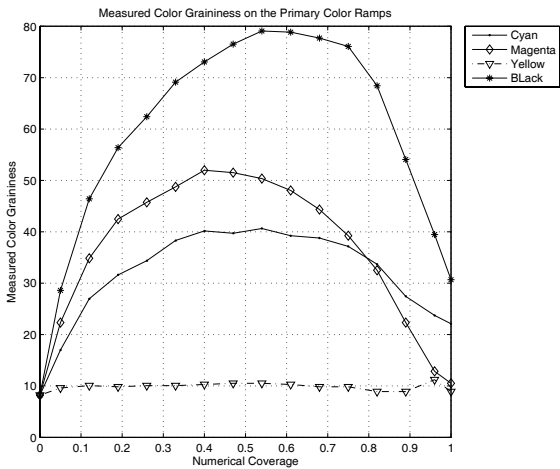


Figure 2. Color graininess along the CMYK ramps

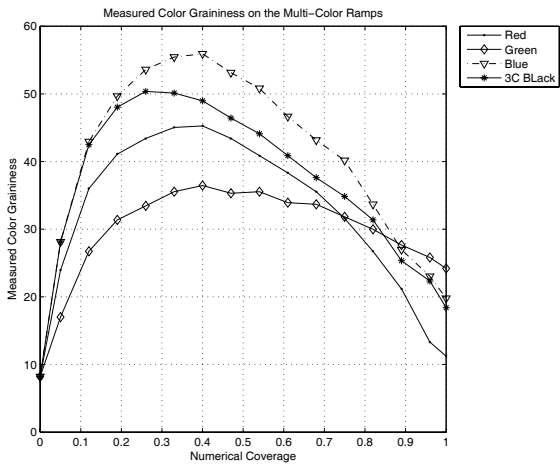


Figure 3. Color graininess along the RGB and 3-color black ramps

printing system. A conventional cluster-dot halftone screen set is chosen during this experiment. Figures 2 and 3 represent the estimated color graininess along the primary CMYK color ramps, secondary RGB color ramps, and CMY neutral color ramp. The luminance differences between CMYK complete coverage area and paper substrate are 45.3, 51.7, 4.6, and 81.2. We can deduce that black and magenta should have higher perceived color graininess than cyan and yellow under the same printing process based on our analysis, which is confirmed in Figure 2. It also shows that the maximal graininess points along the cyan and magenta channel occur near the 50% digital mark, while the maximal graininess point for black is pushed to near the 60% mark. Moreover, the contribution to color graininess through the yellow channel is negligible. Finally, the forward movement of the maximal graininess points along the secondary RGB and CMY neutral color ramps predicted by our previous analysis can be easily seen in Figure 3.

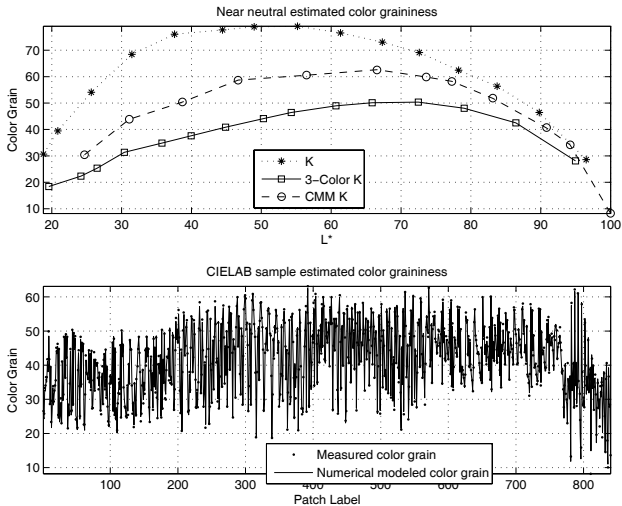


Figure 4. Color graininess along the neutral and CIELAB sampling points

Affine	Quad	Quad/cross	Cubic	Cubic/cross
11%	85%	94%	91%	96%

Because almost all images are composed by multiple colorants, the color graininess performance of a printing system is better described by the graininess derived from the *CIELAB* patches. Table 1 shows the R^2 statistics of different degrees of multivariable polynomial regression correlating between *CIELAB* within the printer gamut and the associated color graininess. The significant improvement in regression accuracy from the first order affine functional to the quadratic functional suggests that dot/hole periphery greatly affects the overall color graininess, and a quadratic functional with all cross terms is the best choice for global graininess modeling striking a balance between the functional complexity and prediction accuracy. The first graph in Figure 4 indicates that different black replacement strategies will affect the performance of a printing system in neutral color graininess. The second graph illustrates that our proposed hybrid nu-

merical graininess model is able to satisfactorily predict color graininess within the printer gamut.

Figures 5 and 6 are two cross sections of the color graininess profile at $L^* = 96$ and $L^* = 68$ in relative colorimetry. Figure 5 shows that the color graininess along the yellow axis is relatively small, but it rises rapidly when other colorants co-exist with yellow colorant. The cross section at $L^* = 68$ indicates that neutral and blue sections of the color gamut produce higher color graininess than other regions.

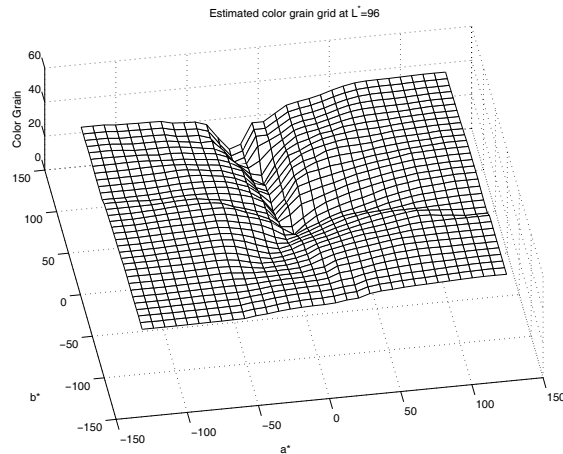


Figure 5. Color grain profile sliced at $L^* = 96$

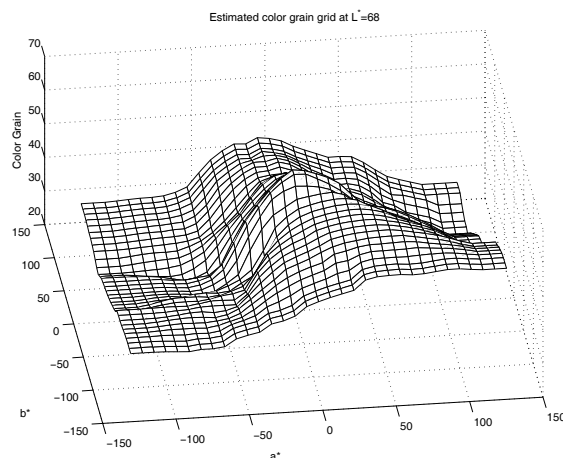


Figure 6. Color grain profile sliced at $L^* = 68$

Conclusion and Future Works

A grain profile is proposed to describe the performance of a printing system in color graininess. We first decompose the perceived color graininess into substrate graininess ζ_s , solid area graininess ζ_a , and halftone dot/hole periphery roughness $g(N_p(R))$ as shown in Equation (5). We propose a hybrid graininess numerical modeling algorithm combining a quadratic multi-variable polynomial and a generalized regression radial basis networks, and our numerical experiment shows that this algorithm can satisfactorily model the overall color graininess behavior of a printing system. Associated with a printer ICC profile and render-

ing intent, a grain profile of a printing system can be created in the PCS color space characterizing the color graininess appearance.

Our theoretical analysis is based on the assumption that the halftone pattern has no contribution to perceived color graininess. This premise does not hold in general when there exists halftone interference semirandom patterns among different color channels and/or a set of stochastic halftone screen is adopted [1, 6, 8, 9]. We plan to extend our analysis and experiment to include those elements in the future.

Acknowledgments

The authors thank Eric Zeise and Hwai Tai for their advice to conduct this experiment and analysis.

References

- [1] C. Kuo and Y. Ng, The Impact of Halftone Screen on Color Graininess, IS&T NIP22, pg. 454, (2006).
- [2] ISO/TC130, ISO/DIS 15076-1, Image technology colour management - Architecture, profile format, and data structure - Part 1: Based on ICC.1: 2004-10.
- [3] ISO/IEC13660, Information technology-office equipment-measurement of image quality attributes for hardcopy output-Binary monochrome text and graphic images, (2001).
- [4] R. Ulichney, Digital Halftoning, MIT Press, (1987).
- [5] M.D. Fairchild, Color Appearance Model, Second Edition, Wiley, (2005).
- [6] H.R. Kang, Color Digital Halftoning, SPIE/IEEE Press, (1999).
- [7] S. Haykin, Neural Networks, a Comprehensive Foundation, Second Edition, Prentice Hall, (1999).
- [8] Y. Ng, H.T. Tai, C. Kuo, and D.A. Gusev, Advances in Kodak NexPress Digital Printing Technology, IS&T NIP23, (2007).
- [9] T. Mitsa, K.J. Parker, Digital Halftoning Technique using a Blue Noise Mask, J. Op. Soc. Am. A, 9, 11, pg.1920-1929, (1992).

Author Biography

Chunhui Kuo is a Scientist at Eastman Kodak Company. He received his Ph.D. in Electrical and Computer Engineering from the University of Minnesota and joined NexPress division of Eastman Kodak Company in 2001. His research interest is in image processing, image quality, blind signal separation and classification, and neural network applied in signal processing. He is a senior member of IEEE signal processing society and a member of IS&T and SPIE.

Yee S. Ng is a Manager Intellectual Property, GCG, at Eastman Kodak Company. Prior to that, he was Senior Research Associate and Chief Engineer with responsibility for the engine image chain and image quality at NexPress Solutions LLC. He is a Kodak Distinguished Inventor and holds 90 U.S. patents. He is a Fellow of IS&T, a Senior Member of IEEE, and a member of New York Academy of Sciences. He is Project Editor for ISO/IEC 19799 (Gloss Uniformity), and ISO/IEC 24734 (Printer Productivity) and Liaison officer from ISO/IEC JTC1 SC28 (Office Equipment) to ISO/IEC TC130 (Graphics). He was General Chairman of NIP19 and received the Chester Carlson Award from IS&T in 2000.

Di Lai received his BS in Biomedical Electronic Engineering at Xi'an Jiaotong University and a MS from the Center for Imaging Science at the Rochester Institute of Technology in 1999. His research interests are in image processing, color science, and 3D visualization. He joined the NexPress division of Eastman Kodak Company in 1999 as an Imaging Scientist. He has been an IEEE member since 2003.